

Oxadiazolyindazole Sodium Channel Modulators are Neuroprotective toward Hippocampal Neurons

Lisa A. Clutterbuck, Cristina Garcia Posada, Cristina Visintin, Dieter R. Riddall, Barrie Lancaster, Paul J. Gane, John Garthwaite, and David L. Selwood*

The Wolfson Institute for Biomedical Research, University College London, The Cruciform Building, Gower Street, London WC1E 6BT, U.K.

Received September 18, 2008

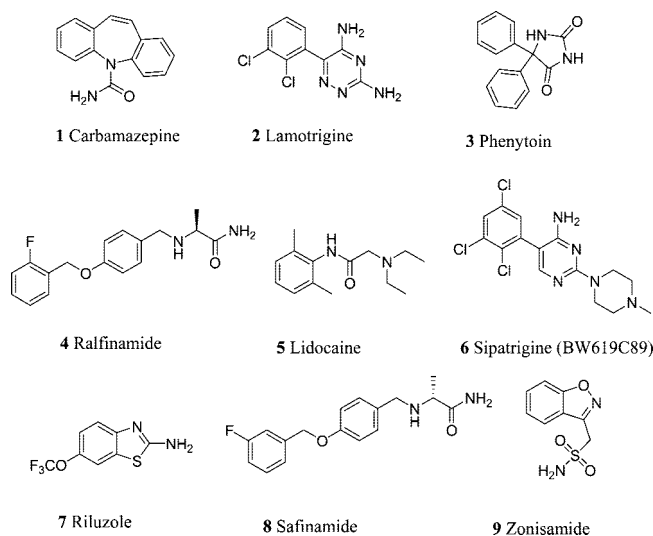
We report the discovery of a new class of neuroprotective voltage-dependent sodium channel modulators exemplified by (5-(1-benzyl-1*H*-indazol-3-yl)-1,2,4-oxadiazol-3-yl)methanamine **11** (CFM1178). The compounds were inhibitors of [¹⁴C]guanidinium ion flux in rat forebrain synaptosomes and displaced binding of the sodium channel ligand [³H]BW202W92. **11** and the corresponding *N*₂-benzyl isomer, **38** (CFM6058), demonstrated neuroprotective activity in hippocampal slices comparable to sipatrigine. CYP450 enzyme inhibition observed with **11** was reduced with **38**. In electrophysiological experiments on dissociated hippocampal neurons, these two compounds caused use- and voltage-dependent block of sodium currents. Sodium channel isoform profiling against Na_v1.1–1.8 demonstrated that the standard sodium channel blocker lamotrigine had modest activity against Na_v1.1, while sipatrigine was generally more potent and less selective. **11** and **38** showed potent activity against Na_v1.6, pointing to pharmacological block of this isoform being consistent with the neuroprotective effect. **38** also showed use dependent block of Na_v1.6 in HEK cells.

Introduction

Voltage-gated sodium channels are found in the cell membranes of electrically excitable cells and are fundamental to the generation of electrical impulses (action potentials). The protein channels exist as heteromers consisting of one pore-forming α -subunit and at least one auxiliary β -subunit¹ with nine isoforms present in nervous or cardiac tissue.² During its normal operation, the channel switches between different functional states: a resting state in which the channel pore is closed; an open state where the channel pore is open and at least two inactivated states where the channel pore is open but nonconducting. Drugs acting on sodium channels are widely used as therapeutic agents in order to treat central nervous system related disorders such as epilepsy and neuropathic pain and, potentially, neurodegeneration associated with ischemic stroke and other conditions (Chart 1).^{3,4} Such drugs often inhibit sodium channels in a manner that is voltage- and use-dependent, properties that suggest interaction with one or more inactivated states. Extensive studies on first generation modulators, carbamazepine **1**, lamotrigine **2**, and phenytoin **3** (all originally anticonvulsants) have led to the design and synthesis of novel derivatives exhibiting more potent activity and selectivity for particular neurological conditions.

Epilepsy, a brain function disorder characterized by the sudden onset of seizures, can be effectively controlled using state-dependent sodium channel modulators,⁴ although at present 30% of patients do not respond to any current drug.⁵ Lamotrigine,⁶ **2**, is widely used as an antiepileptic agent, and carbamazepine, **1**, phenytoin, **3**, and their derivatives oxcarbazepine and fosphenytoin have also proved effective in the treatment of epileptic seizures.⁷ Significant evidence suggests that sodium channels are also involved in the activation of pain pathways,^{8–11} and as a result, many established sodium channel modulators, including anticonvulsants lamotrigine, carbamazepine, and phenytoin have been found to be effective for the

Chart 1. Structures of Sodium Channel Modulators



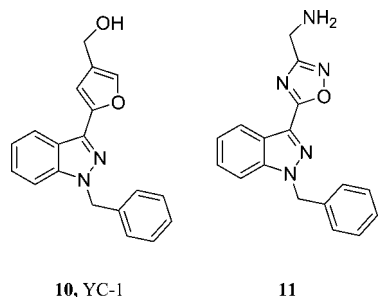
treatment of chronic neuropathic pain.^{12–14} Drugs such as ralfinamide¹⁵ **4** and lidocaine¹⁶ **5** have also shown promising results, while Na_v1.7^a and Na_v1.8 subtype selective compounds are being developed.¹⁷ Although the embryonic Na_v1.3 subtype is expressed in injured neurons, recent studies indicate that it is not implicated in neuropathic pain.¹⁸

It is now well-known that sodium channel modulators are also capable of neuroprotection,¹⁹ a function thought to be useful for reducing brain damage following a stroke, where the brain is deprived of oxygen and glucose.²⁰ As ischemic stroke is the third major cause of death in the Western world,²¹ the development of these compounds has become highly important, especially as there is currently no widely applicable medical treatment available. Nevertheless, many antistroke agents have failed in recent phase II clinical trials,^{22–24} including sipatrigine,

* To whom correspondence should be addressed. Phone: +44 20 7679 6666. Fax: +44 20 7679 0470. E-mail: D.selwood@ucl.ac.uk.

^a Abbreviations: CYP, cytochrome P450; HEK, human embryonic kidney; Na_v, voltage-gated sodium channel.

Chart 2. YC-1 and Its Derivative 11

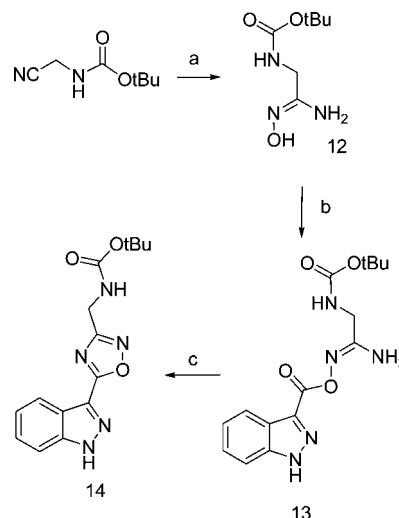


6 (BW619C89),²⁵ because of side effects or lack of efficacy. Although the design of early stroke trials has also been criticized,^{26,27} there is clearly a need for more efficacious compounds with a better side effect profile. Sodium channel modulators may have additional therapeutic utility in chronic neurodegenerative diseases. Riluzole, **7**, in particular, is given to patients with amyotrophic lateral sclerosis,²⁸ and safinamide,²⁹ **8**, and zonisamide, **9**, are both showing promise for improving the motor function in Parkinson's disease. A trial assessing neuroprotection by lamotrigine in secondary progressive MS is currently in progress.³⁰

In a study conducted in 2002 by Garthwaite et al., YC-1 **10**, which is best known as a guanylate cyclase activator, was surprisingly found to inhibit sodium channels in a voltage-dependent manner and was found to protect optic nerve axons from simulated ischemia and from nitric oxide induced toxicity.³¹ This finding led us to investigate analogues of this novel sodium channel modulator for their neuroprotective activity. Protectants for axons are potentially useful in many neurodegenerative conditions, and one sodium channel isoform, Na_v1.6, has been shown to be up-regulated within acute multiple sclerosis lesions³² and to be associated with the loading of demyelinated axons with damaging levels of calcium,¹⁹ indicating its potential as a drug target for neuroprotection. Substitution of the furan ring for an oxadiazole and the hydroxyl moiety for a primary amine yielded compound **11** (CFM1178) (Chart 2). In this paper we report the synthesis and neuroprotective potential of sodium channel modulator neuroprotective analogues of lead compound **11** that show potent blockade of Na_v1.6 and Na_v1.3 isoforms.

Results and Discussion

Design. The design strategy for the library of analogues of sodium channel modulator **11** was based upon one major factor: maintaining or increasing the neuroprotective activity. However, as a secondary aim, it was also beneficial to decrease the potent 2D6 and 1A2 cytochrome P450 enzyme inhibition observed with this compound (see below). From suggested pharmacophore models^{33,34} it appears that the common feature of a large set of sodium channel modulators is the presence of at least one lipophilic group (in our case, possibilities include the benzyl ring, the indazole backbone, or the oxadiazole) and a hydrogen bond donor (the amino group). A recent publication has shown that a series of 3- and 5-aryl-1,2,4-oxadiazoles exhibit anticonvulsant activity in the maximal electroshock seizure model in rats,³⁵ so the presence of this functionality in sodium channel ligands is not unknown. In this study we focused on the modification of the benzyl ring by the addition of a range of lipophilic, hydrophilic, and heteroaryl substituents onto varying positions of the ring. The substituents were chosen to exclude reactive groups,³⁶ according to their lipophilic and electronic

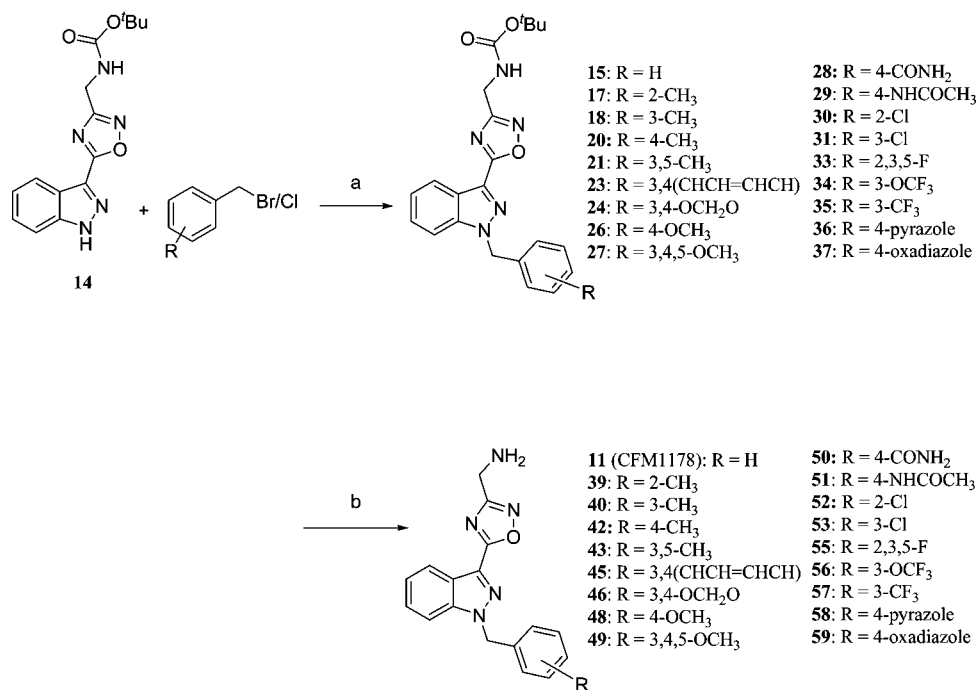
Scheme 1. Synthesis of 1, 2, 4-Oxadiazole Intermediate 14^a

^a Reagents and conditions: (a) hydroxylamine hydrochloride, Na₂CO₃, MeOH, H₂O; (b) indazole-3-carboxylic acid, CDI, DMF; (c) microwave, 140 °C, 20 min.

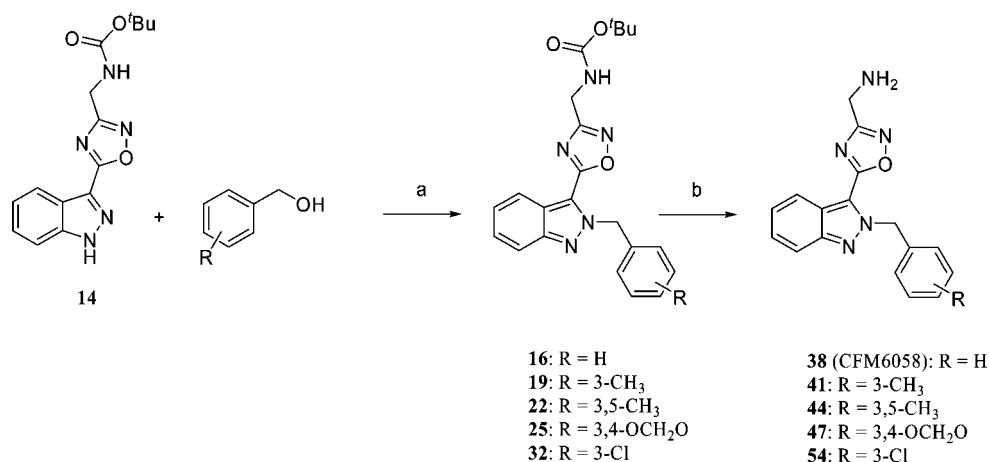
character,³⁷ as well as taking reasonable interpretations of drug likeness³⁸ on the final drug structures into account.

Chemistry. The route to synthesizing the oxadiazole series is shown (Scheme 1).³⁹ The reaction of *N*-(*tert*-butoxycarbonyl)-2-aminoacetamide,⁴⁰ synthesized from hydroxylamine hydrochloride and *N*-(*tert*-butoxycarbonyl)-2-aminoacetone nitrile, with indazole-3-carboxylic acid in the presence of peptide coupling reagent carbonyldiimidazole gave *O*-acylated amidoxime **13** in 93% yield. The subsequent microwave cyclization at 140 °C, in the presence of sodium carbonate, gave the 1,2,4-oxadiazole **14** in 74% yield.^{41,42} The indazole of compound **14** could then be alkylated with substituted benzyl halides, using cesium carbonate as a base, to afford the library of analogues of oxadiazole **11**, with yields of up to 92% (Scheme 2). During the preparation of this library, it was observed by LC-MS and ¹H NMR studies that isomers were being formed, with LC-MS ratios ranging from approximately 1:1 to pure isomer depending on the type of substitution on the benzyl halide. It was discovered that the isomers could be separated easily using flash column chromatography. Thus, after separation of compounds **11** and **38** (CFM6058) ¹H-¹H NOESY NMR experiments revealed the structures to be *N*₁- (major product) and *N*₂-benzyl substituted isomers, respectively. It was subsequently discovered that a modified Mitsunobu⁴³ reaction, using *N,N,N',N'*-tetramethylazodicarboxamide and tributylphosphine, could also be used as a higher yielding route for the preferential synthesis of a number of *N*₂-benzyl substituted indazoles (as shown in Scheme 3), in up to 65% yield. The *tert*-butyl carbamate (Boc) protecting groups of compounds **15**–**37** were then removed to afford the H-donor amino group, using trifluoroacetic acid, triisopropylsilane, and water.

In order to further explore the significance of the hydrophobic benzyl moiety, the synthesis of both Boc-protected and free amine analogues was achieved by *N*₁- and *N*₂-alkylation (Schemes 4 and 5), *N*₁-sulfonylation (Scheme 4), and *N*₁-acetylation (Scheme 6) of indazole **14**. The free amine **68** was also synthesized, without substitution in the *N*₁-position, by deprotecting the Boc group of compound **14** (Scheme 4). We also investigated the effect on the biological activity of carbamate, amide, and sulfonamide derivatives of the primary amine (Scheme 7) by protecting with a benzyl carbamate (Cbz)

Scheme 2. Synthesis of N₁-Benzylated Analogues of Lead Compound 11^a

^a Reagents and conditions: (a) Cs₂CO₃, DMF; (b) TFA, TIPS, H₂O.

Scheme 3. Mitsunobu Synthesis of N₂-Benzylated Analogues of Compound 11^a

^a Reagents and conditions: (a) tributylphosphine, *N,N,N',N'*-tetramethylazodicarboxamide (TMAD), PhMe; (b) TFA, TIPS, H₂O.

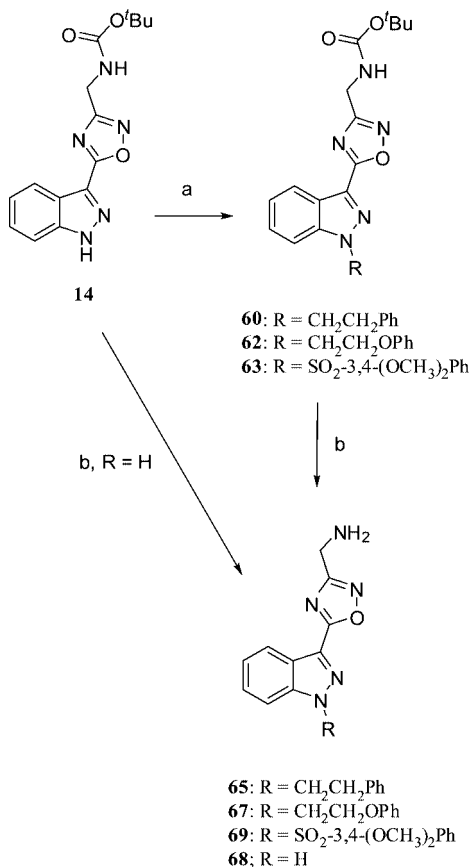
group, using benzyl chloroformate in aqueous solution (pH 8), a benzamide group, using benzoic acid 2-(7-aza-1*H*-benzotriazole-1-yl)-1,1,3,3-tetramethyluronium hexafluorophosphate and diisopropylamine, and a sulfonamide group, using benzene-sulfonyl chloride in aqueous solution (pH 8).

Biological Assays. Both the *tert*-butyl carbamate compounds and the corresponding free amine analogues were evaluated in preliminary assays to ascertain their activity against sodium channels. A radioactive flux assay using the neurotoxin veratridine was used to stabilize the channels of rat forebrain synaptosomes in the open state, allowing [¹⁴C]guanidinium ions to flow through the channel and accumulate within the synaptosomes. Inhibition of this flux on addition of test compounds⁴⁴ served as a “filter” to identify agents with sodium channel blocking activity but is not predictive of neuroprotection. Selected compounds were also screened in a radioligand displacement assay using [³H]BW202W92,⁴⁵ which binds potently to brain synaptosomes, the binding site appearing to

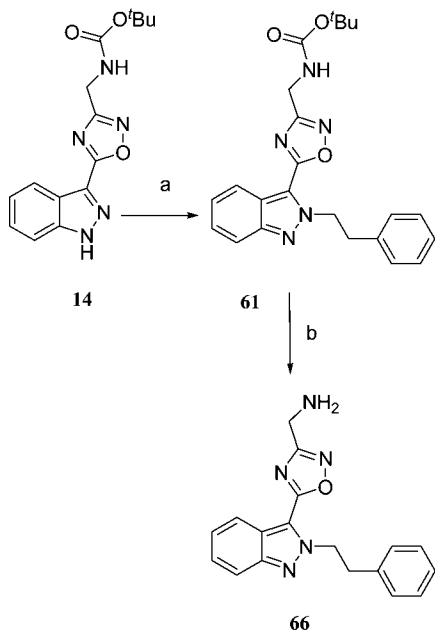
be a pharmacologically relevant site on sodium channels. The neuroprotective activity of the compounds was determined using a hippocampal slice assay, a model for neurodegeneration in which neuroprotective compounds maintain ATP concentrations for longer after the inhibition of glycolysis.⁴⁶ Electrophysiology was utilized to examine the effects of the compounds on channel function in rat hippocampal neurons.³¹ Na_v isoform profiling was conducted using cloned channels expressed in HEK 293 cells. Activity was measured using voltage sensitive dyes (Molecular Devices) and/or patch clamp.

Activity against Sodium Channels and Neuroprotection. As seen from Table 1, the guanidine flux inhibition by *tert*-butyl carbamate protected analogues gave encouraging results with potent activity against sodium channels (IC₅₀ values ranging from 0.4 to 24 μM). Only four compounds, 16, 19, 27, and 30, gave IC₅₀ values greater than 150 μM.

The neuroprotective activities of the compounds, assessed using an *in vitro* hippocampal slice assay, were grouped

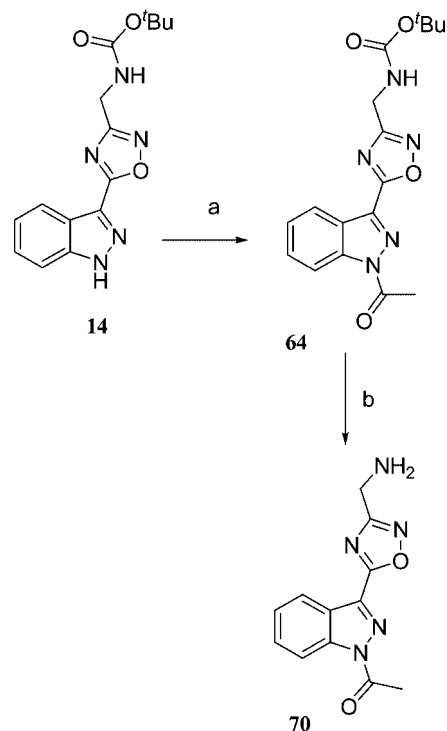
Scheme 4. Synthesis of N_1 -Substituted Compounds^a

^a Reagents and conditions: (a) R-bromide/chloride, Cs₂CO₃, DMF; (b) TFA, TIPS, H₂O.

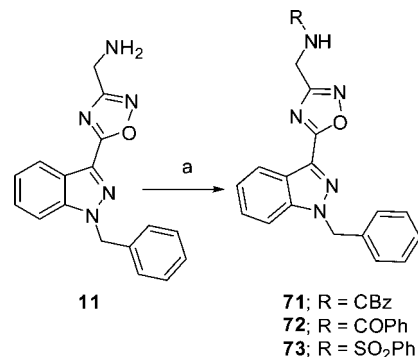
Scheme 5. Synthesis of N_2 -Substituted Compound **61** and **66**^a

^a Reagents and conditions: (a) 2-phenylethanol, tributylphosphine, TMAD, PhMe; (b) TFA, TIPS, H₂O.

according to their percentage neuroprotective activities: not active (0–15%), moderate activity (15–60%), and good activity (>60%). Thus, with no substitution on the benzyl ring, moderate activities of 19% and 25% at 50 μ M were observed for N_1 - and

Scheme 6. Synthesis of N_1 -Acetyl Compound **70**^a

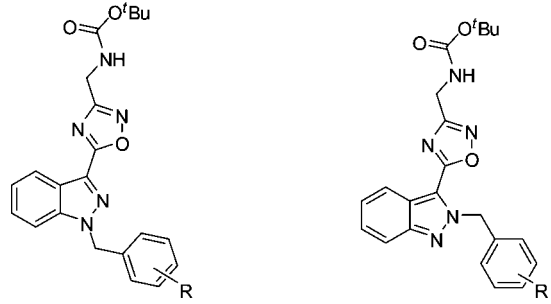
^a Reagents and conditions: (a) Ac₂O, Py, DMAP, CH₂Cl₂; (b) TFA, TIPS, H₂O.

Scheme 7. Synthesis of Carboxybenzyl, Benzamide, and Sulfonamide Analogues of **11**^a

^a Reagents and conditions: (a) PhCH₂COCl, Na₂CO₃ for **71**, PhCOOH, 2-(7-aza-1*H*-benzotriazole-1-yl)-1,1,3,3-tetramethyluronium hexafluorophosphate (HATU) for **72**, PhSO₂Cl, Na₂CO₃ for **73**.

N_2 -isomers **15** and **16** (where R = H). However, it was found that adding a wide range of substituents to the 3, 4, and/or 5 position of the benzyl ring caused a decrease in activity (0–12%). Interestingly, compounds with substituents where R = 4-pyrazole **36**, 4-CONH₂ **28**, and 4-NHCOCH₃ **29** gave similar moderate neuroprotective activities (20%, 29%, and 47%, respectively) to the unsubstituted benzylated indazoles **15** and **16**. It was postulated that protection of the NH₂ hydrogen bond donor moiety with the Boc group could be detrimental to the neuroprotective activity of the compounds. Compounds **28** and **29** could restore some activity by providing NH donors to the active site, though presumably they do not bind in the same orientation.

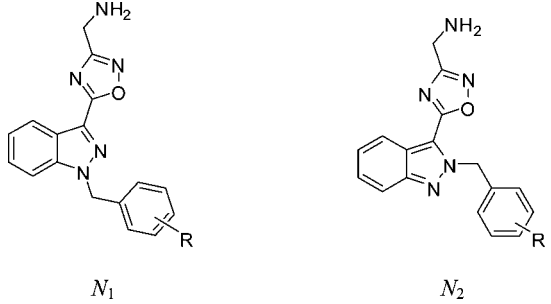
Interestingly, the inhibition of guanidinium ion flux was, on average, slightly less with the free amine analogues than the Boc-protected compounds, with IC₅₀ values ranging from 14–63 μ M (Table 2). N_1 -Benzylindazoles containing more hydrophilic

Table 1. Sodium Channel Modulatory and Neuroprotective Activity of Boc-Protected Analogues of **11**


compd	R (isomer) ^a	neuroprotection at 50 μM (%)	guanidine flux, IC ₅₀ (μM)
lamotrigine		33 ^b	219 ± 22 (13) ^c
tetrodotoxin		100 ^d	
BW202W92		93 ^e	2.6 ± 0.4 (3) ^c
sipatrigine		57 ± 6 (8) ^b	21
15	H (N ₁)	19	5
16	H (N ₂)	25	174
17	2-CH ₃	0	3
18	3-CH ₃ (N ₁)	0	1
19	3-CH ₃ (N ₂)	0	151
20	4-CH ₃	0	2
21	3,5-CH ₃ (N ₁)	0	4
22	3,5-CH ₃ (N ₂)	0	12
23	C ₆ H ₅	0	0.4
24	3,4-OCH ₂ O (N ₁)	0	1
25	3,4-OCH ₂ O (N ₂)	0	3
26	4-OCH ₃	0	4
27	3,4,5-OCH ₃	0	195
28	4-CONH ₂	29	24
29	4-NHCOCH ₃	47	15
30	2-Cl	9	>300
31	3-Cl (N ₁)	12	4
32	3-Cl (N ₂)	0	4
33	2,3,5-F	0	1
34	3-OCF ₃	0	0.9
35	3-CF ₃	3	8
36	4-pyrazole	20	16
37	4-oxadiazole	0	1

^a If not stated, analogue is N₁-isomer. ^b Tested at 30 μM. ^c Mean ± sem (n). ^d TTX tested at 1 μM. ^e Tested at 3 μM.

groups, where R = 3,4,5-OCH₃ **49**, 4-CONH₂ **50**, and 4-NHCOCH₃ **51**, gave greater IC₅₀ values of 178 μM or more. The average neuroprotective activity of the amine series (39%) was over 5 times higher than for the Boc-protected library (7%). This was significant evidence for the importance of the free amine NH-donor in the active site. The highest activities were observed with **11** and the corresponding N₂-isomer **38** (>99% and 63% at 50 μM, respectively). This degree of protection was comparable with that of neuroprotective sipatrigine, **6**, which gave on average 62% at 30 μM in the same assay. Unfortunately, the addition of a range of substituents onto the benzyl ring did not cause any increase in activity, with only similar or lower neuroprotection observed. It could be that the pocket of interaction on the sodium channel may be so specific in size for the hydrophobic benzyl ring that it does not tolerate any substituent except hydrogen. It can be seen, however, that the addition of more hydrophobic substituents or indeed substituents with hydrophobicity close to that of hydrogen (R = 2,3,5-F, 3-CF₃, 3-Cl, 2-CH₃, 4-OCH₃, etc.) onto the benzyl ring, whether electron-withdrawing or donating in nature, allows moderate neuroprotective activity (26–59%). Amines exhibiting very low to zero activity in the assay appeared to be compounds with more hydrophilic substituents on the benzyl rings. For example,

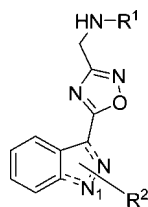
Table 2. Sodium Channel Modulatory and Neuroprotective Activity of Analogues of **11**


compd	R (isomer) ^a	neuroprotection at 50 μM (%)	guanidine flux, IC ₅₀ (μM)
tetrodotoxin		100 ^d	
sipatrigine		57 ± 6 (8) ^b	21
11	H (N ₁)	>99 ± 7 (4) ^c	17.5 ± 1.0 (6) ^c
38	H (N ₂)	63 ± 4 (4) ^c	44.2 ± 2.1 (2) ^c
39	2-CH ₃	46	26
40	3-CH ₃ (N ₁)	45	28
41	3-CH ₃ (N ₂)	37	26
42	4-CH ₃	34	17
43	3,5-CH ₃ (N ₁)	43	15
44	3,5-CH ₃ (N ₂)	35	14
45	C ₆ H ₅	11	20
46	3,4-OCH ₂ O (N ₁)	44	30
47	3,4-OCH ₂ O (N ₂)	55	34
48	4-OCH ₃	35	38
49	3,4,5-OCH ₃	28	178
50	4-CONH ₂	8	195
51	4-NHCOCH ₃	10	309
52	2-Cl	43	20
53	3-Cl (N ₁)	50	14
54	3-Cl (N ₂)	17	24
55	2,3,5-F	59	35
56	3-OCF ₃	33	26
57	3-CF ₃	58	26
58	4-pyrazole	26	63
59	4-oxadiazole	0	58

^a If not stated, analogue is N₁-isomer. ^b Tested at 30 μM. ^c Mean ± sem (n). ^d Tetrodotoxin tested at 1 μM.

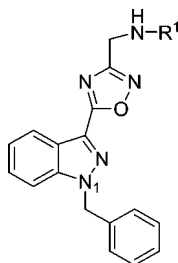
analogues **50** (R = 4-CONH₂) and **51** (R = 4-NHCOCH₃) gave just 8% and 10%, respectively. Sterically bulky substituents also appeared to be disadvantageous to the neuroprotective activity of the amines. Compound **45** (R = C₆H₅), although hydrophobic in nature, gave just 11% neuroprotection, and compound **59**, which contains a methyl oxadiazole in the para-position of the benzyl group, was found to be inactive. Another analogue with a 4-pyrazole substituent **58** also gave a moderate activity of 26%. This further supports the hypothesis that the hydrophobic binding pocket on the sodium channel is precisely defined, which may only allow for hydrophobic groups of a specific size, such as the benzyl group.

In order to further explore the significance of the hydrophobic benzyl moiety, a study involving variation of this group was carried out, as illustrated (Table 3). As expected, the protection of the free amine with the Boc group resulted in inactive compounds (**14**, **60–64**) in the hippocampal slice assay (0–10% neuroprotection), regardless of the nature of the group in the N₁/N₂-position. However, as established previously, the neuroprotective activity was found to return with the NH₂ group to varying degrees depending on the type of substituent in the N₁/N₂-position. The addition of an extra methylene in the chain of the N₁-benzyl substituent, to give compound **65**, gave a moderate neuroprotective activity (49%) compared to **11** (>99%) but similar to sipatrigine, **6** (57%), indicating that a less flexible alkyl chain could be advantageous. The corresponding N₂-

Table 3. Sodium Channel Modulatory and Neuroprotective Activity of Boc-Protected and Free Amine N_1 - and N_2 -Alkylated Indazoles

compd	R ₁	R ₂ (isomer) ^a	neuroprotection at 50 μM (%)	guanidine flux, IC ₅₀ (μM)
60	COO ^t Bu	CH ₂ CH ₂ Ph (N ₁)	0	5
61	COO ^t Bu	CH ₂ CH ₂ Ph (N ₂)	0	85
62	COO ^t Bu	CH ₂ CH ₂ OPh	8	6
14	COO ^t Bu	H	0	96
63	COO ^t Bu	SO ₂ -3,4-OCH ₃ Ph	10	2
64	COO ^t Bu	COCH ₃	4	132
65	H	CH ₂ CH ₂ Ph (N ₁)	49	35
66	H	CH ₂ CH ₂ Ph (N ₂)	54	19
67	H	CH ₂ CH ₂ OPh	40	30
68	H	H	10	2188
69	H	SO ₂ -3,4-OCH ₃ Ph	2	102
70	H	COCH ₃	24	>300

^a Unless otherwise stated, analogue is N_1 -isomer.

Table 4. Sodium Channel Modulatory and Neuroprotective Activity of NH₂-Protected Analogues of Compound **11**

compd	R ₁	neuroprotection at 50 μM (%)	guanidine flux, IC ₅₀ (μM)
11	H	>99	28
15	COO ^t Bu	19	5
71	COOCH ₂ Ph	12	5
72	COPh	23	18
73	SO ₂ Ph	20	5

isomer, **66**, gave an analogous result (54%). Incorporating an ether linker into the chain ($R_2 = \text{CH}_2\text{CH}_2\text{OC}_6\text{H}_5$), to give compound **67**, also gave a moderate activity of 40%. For these hydrophobic compounds, the guanidinium ion flux inhibition IC₅₀ values (19–35 μM) were similar to those of **11** (28 μM). Evidence of the importance of the hydrophobic benzyl substitution in the N_1 -position of the indazole was supplied when the group was removed to leave $R_2 = \text{H}$, **68**. With this modification, the neuroprotective activity fell close to zero. As well as this, guanidinium ion flux inhibition was substantially reduced with compound **68** having an IC₅₀ of 2188 μM in comparison to **11**, which is a potent guanidine flux inhibitor (IC₅₀ = 28 μM). Poor neuroprotective activities were also observed when the benzyl group was substituted for a sulfonyl moiety ($R_2 = 3\text{-SO}_2\text{-3,4-OCH}_3\text{Ph}$) and an acetyl group ($R_2 = \text{COCH}_3$), with compounds **69** and **70** giving just 2% and 24%, respectively. Again, the inhibition of guanidinium ion flux of both these compounds was low with IC₅₀ values of 102 and >300 μM, respectively.

In addition to these data, Table 4 demonstrates that acylation or sulfonylation of the free amine is damaging to the neuroprotective activity of analogue **11**. The benzyl carbamate (Cbz) and phenyl amide (Scheme 7) gave similar activities of 12%

and 23% compared with the *tert*-butyl carbamate group (19%), well below the value for the unprotected compound **11** (>99%). Despite this, the compounds still appear to be sodium channel modulators as evidenced by their activities in the guanidinium flux assay.

Pharmacophore and Quantitative Structure–Activity Studies. A three-point pharmacophore for sodium channel blockers with anticonvulsant activity has been described by Unverferth et al.³⁴ The essential features of a number of compounds, which includes the neuroprotectant lamotrigine, appear to be a hydrophobic unit, in most cases an aromatic ring, an electron donor, and a hydrogen bond donor–acceptor. With this in mind, we compared our neuroprotective free amine series (Table 2) with Unverferth's pharmacophore to discover if the same features existed. Using the overlay of N_1 -isomer **11** with sipatrigine **6** (Figure 1a) while taking into account the number of available electron donors present, it was possible to identify all the required pharmacophore points closely matching the distance criteria. In order to optimize the pharmacophore distances, we defined the nitrogen of the indazole of **11** as the electron donor group (D) (Figure 1a), which gave a distance to the hydrogen bond acceptor–donor (HAD) unit within the specified range (3.9–5.5 Å). The HAD to hydrophobic unit (R) distance (4.2–8.5 Å) and the D to R distance (3.2–5.1 Å) were also found to be well within the distance limits suggested by Unverferth.

In an attempt to investigate whether we could find any correlation between QSAR descriptors and the current neuroprotectant data (Table 2), all MOE (MOE 2006.09) descriptors (2D, i3D, and 3D) were calculated; these were then plotted on a correlation matrix. Correlation values range from 1 to ±100. High correlation exists when the figures are closer to 100 or –100. Overall, 31 of the calculated descriptors had a correlation with the neuroprotectant data of greater than ±55. When the compute QuaSAR model was run within MOE⁴⁷ using all the above descriptors, the relative importance of each descriptor was identified. Cross-validating the model presents a QSAR equation to model the activity data. The QSAR analysis was rerun with the top 10 selected descriptors, and we compared the predicted activities with the known neuroprotective activity data of the analogues (Table 2), which gave a correlation coefficient (r^2) of 0.70. The correlation plot of measured activity versus predicted activity is shown in Figure 1b. Using PCA (principal component analysis), a small set of descriptors was selected: ASA (water accessible surface area calculated using a radius of 1.4 Å for the water molecule), b_count (number of bonds), diameter, vol (van der Waals volume), vsa_acc (surface area of H-bond acceptors), vsa_pol (surface area of polar atoms), and weinerPath (the sum of bond distances between all heavy atom pairs in the molecule, an adjacency and distance matrix descriptor). Most of the variance (96.7%) was covered by the first three principal components (PC). From a plot of the first three PC described above (Figure 1c), the active compounds (green spheres defined as having a neuroprotective activity of >30%) are clustered mostly in the center and those with activity below this are scattered randomly (red spheres). Unexpectedly, however, the N_2 -analogue **54** (where R = 3-Cl), which according to our predictive model ought to be active and found in the central cluster, was actually found to have a low activity of 17%. Other factors not captured by this QSAR may be responsible for the poor activity of this compound. In fact, the binding displacement IC₅₀ of this compound was found to be 110 μM compared to that of its N_1 -derivative, which was just

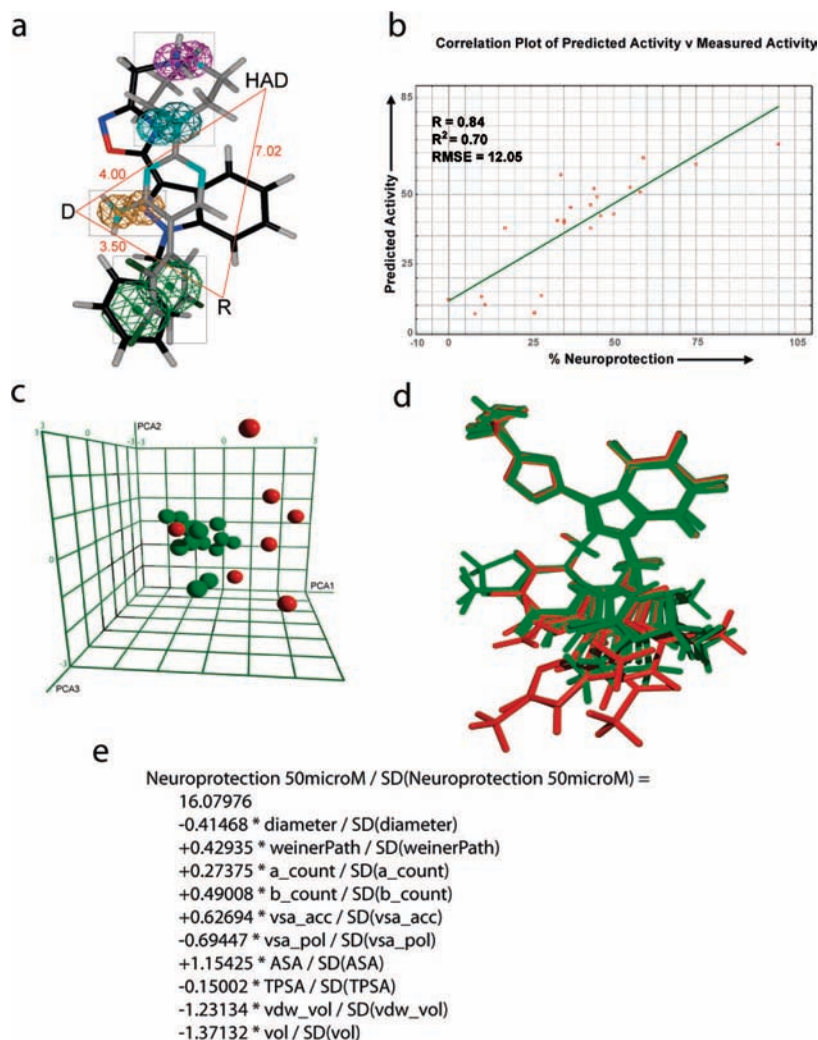


Figure 1. (a) Superposition of **11** (black, carbon; dark-blue, nitrogen; red, oxygen) and sipatrigine, **6** (gray, carbon; cyan, nitrogen), showing the matching pharmacophore points, HAD (hydrogen bond acceptor/donor, cyan/magenta), D (electron donor, orange), and R (hydrophobic/aryl unit, green). Distances are in angstroms. (b) QSAR correlation plot of predicted versus measured activity (% neuroprotection in μM). (c) A 3D plot of the first three principal components from the QSAR analysis. All free amine analogues (Table 2) are shown as spheres. Those colored green represent activity greater than 30%, and those colored red have activity less than 30%. (d) Superposition of the free amine series (Table 2). Those in green have activity greater than 30%, and those in red have activity less than 30%. (e) Estimated normalized linear model for the 10 selected descriptors.

3 μM . This may indicate a steric clash for this compound in the binding site.

In conclusion, from the overlay of the free amine series (**11**, **38**–**59**) as shown in Figure 1d, it can be observed that extending the N_1 - and/or N_2 -benzyl substituent greater than 8 Å will markedly reduce activity. The QSAR descriptors, which most correlate with neuroprotective activity, are inversely related to size/shape and lipophilicity. Thus, the greater the volume or the surface area is, the less active the compounds become. In this series, charge effects seem to be negligible, which suggests that there is a defined pocket in terms of dimensions for the substituent and which is probably hydrophobic or weakly polar.

Electrophysiological Studies in Rat Hippocampal Neurons.

An electrophysiological assessment of the activity of compounds was undertaken using neurons that were acutely isolated from the rat hippocampus. The aim was to determine if the activity of compounds against sodium channels showed use- or voltage-dependence, which is characteristically shown by many drugs active against sodium channels.⁴⁸

The voltage- and use-dependent action of **38** on sodium currents in hippocampal neurones is illustrated in Figure 2. The

peak sodium current evoked by voltage steps to different membrane potentials produces the current–voltage relationships (Figure 2a,b). The difference between the two graphs is in the initial membrane potential: -90 mV (Figure 2a) and -70 mV (Figure 2b). The inhibitory action of 30 μM **38** is $\sim 10\%$ at -90 mV compared to $\sim 60\%$ at -70 mV. This effect was reversible upon washout (data not shown). Frequency- or use-dependence was examined using a 20 Hz train of 20 voltage steps from -90 mV. The duration of the step was 3.5 ms in panel c and 20 ms in panel d (Figure 2). Under control conditions, peak currents during the train showed a mild cumulative depression that was slightly greater with the longer duration steps. This is probably the result of the recruitment of the slow inactivated state of sodium channels, which becomes greater with longer duration voltage steps. Correspondingly, the cumulative inhibition of peak current in the presence of 30 μM **38** was also much greater with 20 ms than with 3.5 ms voltage steps.

An additional test for a preferred drug action on slow inactivation is a paired pulse protocol in which a 300 ms conditioning voltage step to 0 mV (from -90 mV) is followed

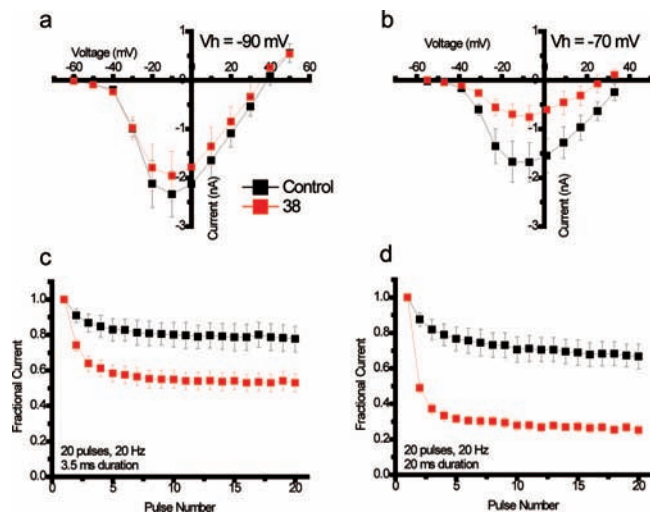


Figure 2. Voltage- and use-dependent action of **38** on Na^+ currents from a single neuron. Initial membrane potentials were -90 mV (a) and -70 mV (b). **38** at $30 \mu\text{M}$ is inhibitory at $\sim 10\%$ at -90 mV compared to $\sim 60\%$ at -70 mV. Frequency- or use-dependence was examined using a 20 Hz train of 20 voltage steps from -90 mV. The duration of the step was 3.5 ms (c) and 20 ms (d). Under control conditions, peak currents show a mild cumulative depression during the train that is slightly greater with the longer duration steps. The cumulative inhibition of peak current in the presence of $30 \mu\text{M}$ **38** is also much greater with 20 ms than with 3.5 ms voltage steps.

by a return to -90 mV for 15 ms before a second, test, voltage step for 10 ms to 0 mV. The 300 ms conditioning pulse causes both fast and slow inactivation, while the short interval only allows recovery from fast inactivation. Thus, greater inhibition of the sodium current during the second step indicates that the slow inactivated state is more readily inhibited than the resting state. The inhibition at resting state (Figure 3a, pulse 1 data) is shown compared to the inhibition after development of slow inactivation (pulse 2, hatched bars) for sipatrigine **6**, **38**, and **11**, all at $30 \mu\text{M}$. Both **11** and **38** compounds showed a preferential inhibition of the current produced by the second step, pointing to selectivity for the inactivated state that was similar to that of sipatrigine, which has demonstrated neuroprotective effects.

38 showed use-dependent action (Figure 2c) even when the duration of voltage steps was short enough to minimize the development of slow inactivation. However, when compared to sipatrigine **6** (Figure 3c) and **11** (Figure 3b), it is clear that only **38** (Figure 3d, which repeats Figure 2c for comparison) shares the properties of sipatrigine **6** that are examined here, since **11** has no effect on the sodium currents during short voltage steps. In analogous experiments **38** also showed very similar actions on currents recorded from cell lines expressing $\text{Na}_v1.6$ (data not shown). Progressive inhibition of short duration (3.5 ms) pulses by sipatrigine **6**, but not lamotrigine, has been reported previously.^{49,50} There could be several explanations for the inhibition seen during shorter pulses, for example, direct block, an action on fast inactivation, or a facilitation of entry to the slow inactivated state.

Na_v Isoform Profiling. The availability of the cloned sodium channel isoforms expressed in cell lines allows us to examine the selectivity of our novel neuroprotective agents and to explore the extent to which blockade of each isoform is necessary for neuroprotection. Our neuroprotection assay (hippocampal slice) contains cell bodies, axons, and probably a mix of $\text{Na}_v1.1$, $\text{Na}_v1.2$, $\text{Na}_v1.3$, and $\text{Na}_v1.6$ channels.^{51–54} We utilized two assay methods to assess isoform selectivity: fluorescence readouts

from voltage sensitive dyes (Table 5) as an initial screen at a single concentration ($10 \mu\text{M}$) and follow-up automated electrophysiological patch-clamp investigations on $\text{Na}_v1.2$ and $\text{Na}_v1.6$ (Table 6). Unfortunately voltage-sensitive dye testing of $\text{Na}_v1.2$ was unavailable as was testing of $\text{Na}_v1.9$. For comparison (Table 5) we present the [^3H]BW202W92 binding affinities of the compounds in synaptosomes.⁴⁵ If we examine the standard sodium channel blockers in Table 5, then we can see that the neuroprotective compounds sipatrigine and BW202W92 showed activity against all the isoforms, with BW202W92 showing some evidence of selectivity for $\text{Na}_v1.3$ and $\text{Na}_v1.8$. The anticonvulsant (but weakly neuroprotective agent) lamotrigine also showed little or no selectivity and was relatively less potent than sipatrigine **6** and BW202W92. This is in broad agreement with data reported from other laboratories.^{55,56} This pattern of activity for BW202W92 indicates that the radiolabeled form is capable of sampling all the isoforms present in the hippocampal slice and, therefore, that this ligand may be unsuitable for assessment of neuroprotection activity per se. The potent binding of BW202W92 reflects its activity against all the neuronal isoforms (Tables 5 and 6). The novel neuroprotective agent **11** presented here showed weak $\text{Na}_v1.2$ activity (Table 6) even at $50 \mu\text{M}$. All the neuroprotective compounds showed significant $\text{Na}_v1.6$ activity, and this was confirmed by patch-clamp evaluation (Table 6). The compounds also showed potent activity against the $\text{Na}_v1.3$ isoform. Taken together, the data point to pharmacological block of $\text{Na}_v1.6$ being consistent with the observed neuroprotective activity or, perhaps, simultaneous block of several isoforms may be required. Block of $\text{Na}_v1.2$ does not seem to be key (note the low activity of **11** at $\text{Na}_v1.2$), at least for the hippocampal slice in vitro system. The involvement of $\text{Na}_v1.3$ remains open; this isoform is expressed in adult rat and human hippocampus⁵³ and is up-regulated in response to nerve injury⁵⁷ and in spontaneously epileptic rats.⁵⁴

Cytochrome P450 Activity. Cytochrome P450 (CYP 450) enzymes are responsible for the oxidative metabolism of drugs in animals. The inhibition of this enzyme is undesirable because it could lead to the accumulation of other drugs to toxic levels in the body. Initial studies on lead compound **11** revealed it to have potent inhibition against the CYP2D6 enzyme, which metabolizes approximately 20% of drugs, including antiarrhythmics, antidepressants, and analgesics.^{58,59} Furthermore, the compound caused even greater inhibition of CYP1A2. The secondary aim, therefore, was to try to find a compound with less CYP inhibition than lead compound **11** while still maintaining good neuroprotective activity. A number of Boc-protected and free amine analogues were therefore screened for CYP2D6 and CYP1A2 inhibition, as shown in Table 7. Initially, it was proposed that the hydrophobic nature of N_1 -benzylindazole **11** was the cause of the CYP inhibition, but surprisingly and agreeably, the corresponding N_2 -benzylindazole isomer **38** was found to be a less potent inhibitor of CYP2D6 by approximately 100 times ($\text{IC}_{50} > 10 \mu\text{M}$). It was also in the region of 32 times less inhibiting than **11** for the CYP1A2 enzyme ($0.36 \mu\text{M}$). In fact, it appeared that compound **11** was somewhat irregular, as all other compounds, whether Boc-protected or free bases, gave CYP2D6 inhibition IC_{50} values of between 1.3 and $20 \mu\text{M}$, with Boc-protected analogues in general showing the least CYP inhibition (3.3 – $20 \mu\text{M}$). The free amine indazoles with methyl or CONH_2 substituents on the benzyl rings (**40**, **43**, **50**), however, were found to be more potent inhibitors of CYP2D6, with IC_{50} values ranging from 1.3 to $4.3 \mu\text{M}$. It was noticed that these compounds were also inhibitors of CYP1A2 enzyme,

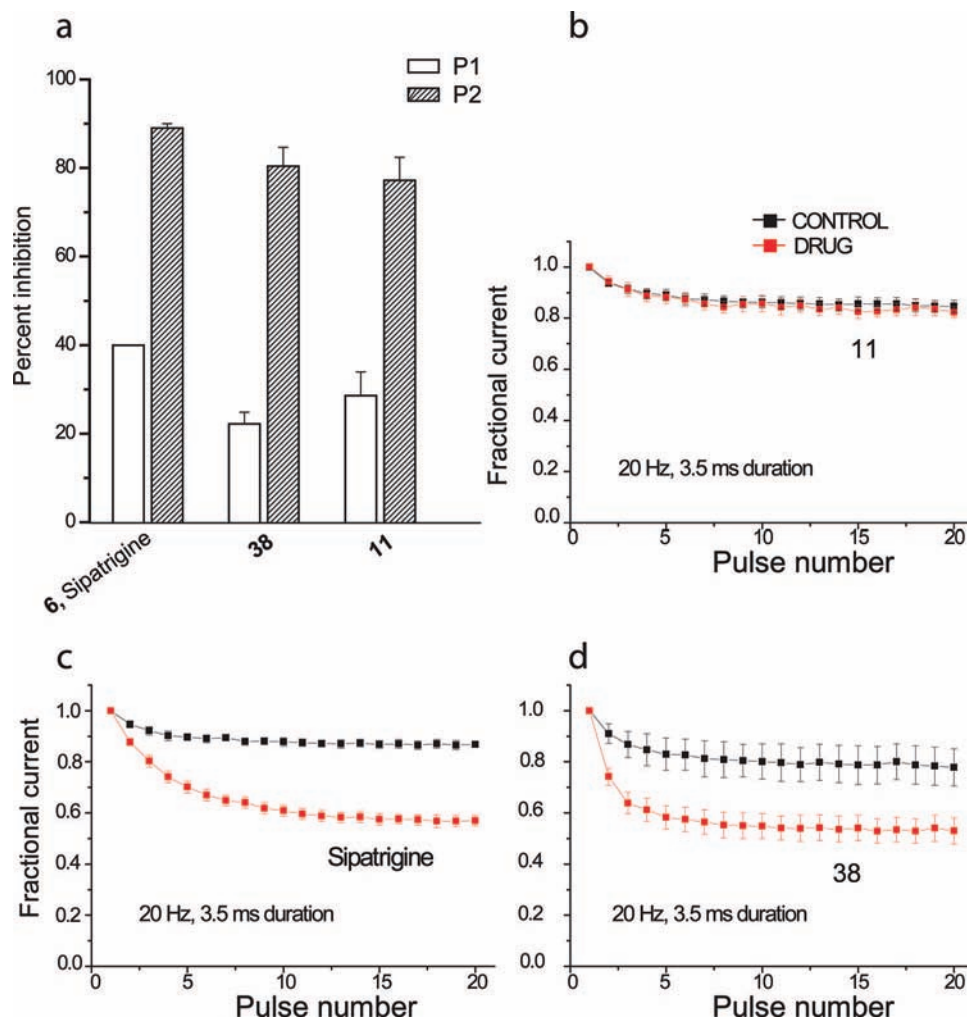


Figure 3. Slow inactivation examined using a paired pulse protocol in which a 300 ms conditioning voltage step to 0 mV was followed by a 15 ms period at -90 mV before a second, test, voltage step. The tonic inhibition observed in response to pulse 1 (P1) is compared to the inhibition during pulse 2 (P2) after the development of slow inactivation for sipatrigine **6**, **38**, and **11**, all at $30 \mu\text{M}$. Compounds **11** and **38** showed a preferential block during P2, signifying preferential activity on the inactivated state, that was equal to or greater than that of sipatrigine. Frequency- or use-dependence was examined for **11** (b), sipatrigine (c), and **38** (d) using a 20 Hz train of 20 voltage steps from -90 mV. The duration of the step was 3.5 ms (panel d repeats Figure 2c and is shown for comparison).

with IC_{50} values ranging from 0.062 to $0.084 \mu\text{M}$. Compound **65** where $\text{R}_2 = \text{CH}_2\text{CH}_2\text{C}_6\text{H}_5$ also gave an IC_{50} of $0.034 \mu\text{M}$, and the corresponding N_2 -isomer, **66**, gave an IC_{50} of $0.36 \mu\text{M}$. Interestingly, of the two cases investigated, N_2 -isomers appeared to be weaker CYP inhibitors than their N_1 -counterparts. Despite the compounds having some CYP1A2 inhibitory activity, this enzyme is only responsible for the metabolism of approximately 3% of drugs, and so its inhibition is not such a major problem as for CYP2D6.

Conclusion

Our screening strategy was directed toward optimizing the functional neuroprotection and state-dependent block by our compounds rather than their potency in the sodium channel assays. Although good selectivity for sodium channel subtypes may be possible (as observed for $\text{Na}_v1.7$ and $\text{Na}_v1.8$),¹⁷ sodium channels are exquisitely regulated, with multiple phosphorylation sites contributing to function.⁶⁰ We therefore considered it important to use assays that measured the desired functional activity (in this case, neuroprotection) of the compounds. Subsequent analysis of the best compounds would help elucidate the precise molecular targets.

The potent CYP2D6 and 1A2 inhibition by lead compound **11** was found to be uncommon in our series of compounds,

and a number of hydrophobic or hydrophilic N -benzyl substituents were weaker inhibitors of the enzymes. Most notable was the N_2 -benzylated isomer of **11** (**38**) which, as well as being a good neuroprotective agent, was 100 times less potent than **11** against CYP2D6.

Our lead free amine, the N_1 -benzylated indazole **11**, and its corresponding N_2 -isomer **38** have neuroprotective activity (>99 and 63%) comparable to that of sipatrigine. It appears that adding substituents, whether they are lipophilic, electron-donating, electron-withdrawing, or heteroaryl groups, to the benzyl ring of **11** or **38** does not increase the neuroprotective activity, although in most cases activity is maintained. Derivatizing the free amine moiety was found to be hugely detrimental to the activity of these compounds, with approximately 5-fold less potency for a series of Boc-protected N -benzylated compounds. Despite this, the series of Boc-protected and free amine derivatives in general were found to be effective sodium channel modulators in both [^{14}C]guanidium ion flux and [^3H]BW202W92 binding assays. It appears also that the hydrophobic benzyl group in the N_1 - or N_2 -position of the indazole is important for neuroprotective activity.

In comparison to sipatrigine **6**, both **11** and **38** were comparable in their action on the slow inactivated state of native

Table 5. Na_v Isoform Screening of Standard and Novel Sodium Channel Blockers against Central (Italic) and Peripheral Sodium Channel Isoforms Compared to BW202W92 Binding^a

compd	³ H]BW202W92 binding, IC ₅₀ (n) (μM)	inhibition (%) (IC ₅₀ in bold (μM))						
		Na _v 1.1	Na _v 1.3	Na _v 1.4	Na _v 1.5	Na _v 1.6	Na _v 1.7	Na _v 1.8
11	3.3 ± 0.6 (5)	48	79	97	48	0.66	59	90
38	6.7 ± 2.8 (2)	51	78	98	81	1.03	92	84
lamotrigine	2.6 ± 0.5 (5)	44	22	21	40	23	45	46
sipatrigine	0.5 ± 0.1 (5)	55	61	97	97	70	67	76
BW202W92	0.04 ± 0.1 (3)	56	100	98	39	37	44	86

^a BW202W92 binding IC₅₀. Change in membrane potential was measured using MP-red voltage sensitive dye. Values are the percentage inhibition at 10 μM (mean values of of duplicates) or IC₅₀ determinations in μM (bold italic).

Table 6. Patch-Clamp Electrophysiology for Na_v1.6 on Selected Compounds^a

compd	concn (μM)	Na _v 1.2 inhibition	Na _v 1.2 use-dependent inhibition	Na _v 1.6 inhibition	Na _v 1.6 use-dependent inhibition
11	10	6.6 ± 1.2	1.9 ± 4.3	9.5 ± 0.5	1.1 ± 0
	50	10.8 ± 11	14.7 ± 6.3	40.9 ± 3.7	18.7 ± 10
38	10	13 ± 1.8	35.8 ± 5.2	10.2 ± 4.0	29 ± 5.2
	50	33.8 ± 4.4	70.8 ± 17	31.5 ± 12	65.8 ± 19
sipatrigine	10	21.6 ± 1.5 ^b	40.1 ± 6.5	10.4 ± 4.0	37 ± 5.7
	50	75.2 ± 21 ^b	84.6 ± 13	43.4 ± 6.6	63.2 ± 11
BW202W92	10	0.7 ± 2.3	43.4 ± 6.9	2.3 ± 1.4	81.4 ± 9
	50	75.2 ± 21	88.5 ± 16	62.7 ± 7.6	97.3 ± 1.2
lamotrigine	30	7.9 ± 2.8	4.1 ± 1.8	NT	NT
	100	17 ± 8.5	18.1 ± 11	NT	NT

^a Results expressed as percentage inhibition at the concentrations shown and are the mean values of duplicate experiments (n = 2) unless otherwise indicated. NT = not tested. ^b n = 3.

Table 7. CYP2D6 and CYP1A2 Inhibition of Boc-Protected and Free-Amine Analogues of **11**^a

compd	R ₁	R ₂ (isomer)	IC ₅₀ (μM)		
			CYP2D6 inhibition	CYP1A2 inhibition	CYP3A4 inhibition
14	COO ^t Bu	H	>10	0.79	
63	COO ^t Bu	SO ₂ -3,4-(OCH ₃) ₂ Ph	20		
64	COO ^t Bu	COCH ₃	>10		
28	COO ^t Bu	CH ₂ Ph-4-CONH ₂	>10		
36	COO ^t Bu	CH ₂ -4-(1-pyrazole)Ph	>10		
29	COO ^t Bu	CH ₂ Ph-4-NHCOCH ₃	13	5.92	
24	COO ^t Bu	CH ₂ 3,4-(OCH ₂ O)Ph	3.3	4.86	
18	COO ^t Bu	CH ₂ -3(CH ₃)Ph	20		
68	H	H	11	0.21	
69	H	SO ₂ -3, 4(OCH ₃) ₂ Ph	2.9	>10	
70	H	COCH ₃	>10		
50	H	CH ₂ Ph-4-CONH ₂	1.3		
43	H	CH ₂ -3,5(CH ₃) ₂ Ph	3.73	0.062	
11	H	CH ₂ Ph (N ₁)	0.09	0.009	3.1
38	H	CH ₂ Ph (N ₂)	>10	0.315	
65	H	CH ₂ CH ₂ Ph (N ₁)	1.32	0.034	
66	H	CH ₂ CH ₂ Ph (N ₂)	4.27	0.36	
40	H	CH ₂ -3(CH ₃)Ph	3.96	0.084	

^a Data obtained on human recombinant YP enzymes.

sodium channels. Sipatrigine **6** has an action even with short depolarization, which was also observed with **38** but not with **11**. Whether this reflects an additional mechanism of action and/or is therapeutically important is unclear. The currents measured in acutely isolated neurons have likely contributions from Na_v1.2 as well as Na_v1.6. Na_v isoform profiling demonstrated little isoform selectivity for the standard sodium channel blockers, lamotrigine and sipatrigine. In contrast **11** lacked Na_v1.2 activity but showed potent Na_v1.6 and evidence of Na_v1.3 activity. Taken together, the data point toward pharmacological

block of Na_v1.6 being important for neuroprotection in our isolated hippocampal slice assay; the involvement of the other isoforms, particularly Na_v1.3, remains to be clarified. Investigations with more selective compounds will be required to confirm if blockade of Na_v1.6 is sufficient to achieve neuroprotection.

Experimental Section

General. All starting materials were either commercially available or synthesized by methods reported in the literature. Reactions were monitored by thin-layer chromatography (TLC) on silica gel plates (60 F₂₅₄, Merck), visualizing with ultraviolet light. Column chromatography was performed on silica gel Si II, Isolute columns. Melting points were determined on a Gallenkamp melting point apparatus and are uncorrected. ¹H and ¹³C NMR spectra were recorded on a Bruker Spectrospin 300 Hz. ¹H NMR chemical shifts are reported in parts per million downfield from tetramethylsilane. Mass spectra were recorded on either a VG ZAB SE spectrometer (EI, FAB) or a Gilson-Finigan AQA LC-mass spectrometer using C-18 column (Hypersil BDS 100 mm × 4.6 mm, 5 μm). Microanalysis was carried out by the Analytical Services Section, Department of Chemistry, University College London. Purification by reverse-phase HPLC (Gilson) used preparative C-18 columns (Hypersil PEP 100 mm × 21 mm, 5 μm). IR spectra were recorded on a Perkin-Elmer Spectrum One series FT-IR spectrophotometer. The microwave experiments were run on a Biotage Initiator 60 microwave. All compounds were at least 95% pure as assayed by LCMS (electrospray +ve).

Synthesis of tert-Butyl 2-Amino-2-(hydroxyimino)ethylcarbamate⁴⁰ (12). To a solution of sodium carbonate (8.5 g, 80 mmol) in water (35 mL) was slowly added a solution of hydroxylamine hydrochloride (5.6 g, 80 mmol) in water (35 mL). The aqueous solution of hydroxylamine was added to a solution of the *N*-(tert-butoxycarbonyl)-2-aminoacetonitrile (12.5 g, 80 mmol) in methanol (200 mL). The clear light-yellow solution was heated at reflux for 23 h with more water (100 mL) added as necessary to dissolve the precipitate formed. The methanol was removed under reduced pressure, and the residue was partitioned between ethyl acetate (100 mL) and water (100 mL). The aqueous phase was extracted with ethyl acetate, and the combined organic phase was dried over magnesium sulfate. The solvent was removed in vacuo to give a white powder (9.8 g, 65%): mp 147–148 °C; δ_H (300 MHz, MeOH-*d*₄) 1.44 (9H, s, O^tBu), 3.64 (2H, s, CH₂); δ_C (75.5 MHz, MeOH-

d_4) 158.8, 154.7, 80.7, 41.4, 28.7; LC-MS-EI 190.2 (MH⁺, 100); found (CI) 190.118 79. C₇H₁₅N₃O₃ (MH⁺) requires 190.119 16.

tert-Butyl 2-(1*H*-Indazole-3-carboxyloxyimino)-2-aminoethyl-carbamate (13). To a round-bottomed flask was added indazole-3-carboxylic acid (21.1 g, 0.13 mol) in dimethylformamide (DMF) (500 mL) under nitrogen. Carbodiimidazole (CDI) (23.2 g, 0.14 mol) was added to the yellow solution and was stirred at room temperature for 30 min. *N*-(*tert*-Butoxycarbonyl)-2-aminoacetamidoxime **12** (27.1 g, 0.14 mol) in DMF (100 mL) was then added, and the solution was stirred for 18 h at room temperature. The solvent was removed in vacuo on a high vacuum pump, and the crude solid was dissolved in dichloromethane. The resulting precipitate was filtered off and dried in vacuo to give a beige powder (39.6 g, 92%); mp 185–186 °C; δ_{H} (300 MHz, MeOH- d_4) 1.47 (9H, s, O'Bu), 3.86 (2H, s, CH₂), 7.33 (1H, t *J* 7.9 Hz, ArH), 7.50 (1H, t *J* 6.9 Hz, ArH), 7.65 (1H, d *J* 8.5 Hz, ArH), 8.23 (1H, d *J* 8.2 Hz, ArH); δ_{C} (75.5 MHz, DMSO- d_6) 161.3, 157.6, 155.8, 140.8, 134.9, 126.6, 122.6, 122.1, 121.1, 110.9, 78.4, 40.9, 28.1; LC-MS-EI (MH⁺, 100); found (FAB) 356.132 84. C₁₅H₁₉N₅O₄Na (M + Na) requires 356.133 47.

3-[3-*tert*-Butoxycarbonylaminoethyl-1,2,4-oxadiazol-5-yl]indazole (14). Boc-protected O-acylated amidoxime (**13**) (2.0 g, 6mmol) was added to a 20 mL microwave vial with DMF (12 mL) and sodium acetate (0.54 g, 6.6 mmol). The microwave reaction mixture was heated to 140 °C for 20 min with stirring. The solvent was then removed in vacuo on a high vacuum pump, and the remaining crude yellow solid was dissolved in dichloromethane (100 mL) and washed with water (100 mL), sodium hydrogen carbonate (aq) (100 mL), 1 N HCl (aq) (100 mL), and brine (100 mL). The organic phase was then dried over magnesium sulfate and the solvent removed in vacuo to give a white powder (1.48 g, 78%); mp 169–170 °C; δ_{H} (300 MHz, MeOH- d_4) 1.47 (9H, s, O'Bu), 4.55 (2H, s, CH₂), 7.36 (1H, t *J* 6.9 Hz, ArH), 7.53 (1H, t *J* 5.9 Hz, ArH), 7.68 (1H, d *J* 8.5 Hz, ArH), 8.26 (1H, d *J* 7.3 Hz, ArH); δ_{C} (75.5 MHz, MeOH- d_4) 172.6, 158.3, 142.6, 131.8, 128.7, 124.4, 122.9, 121.9, 111.9, 80.8, 37.4, 28.7; LC-MS-EI 316.2 (MH⁺, 100); found (FAB) 316.140 04 C₁₅H₁₇N₅O₃ (MH⁺) requires 316.140 96. Anal. Calcd for C₁₅H₁₇N₅O₃: C, 57.13; H, 5.43; N, 22.21. Found: C, 57.51; H, 5.51; N, 21.83.

General Method for the Synthesis of the N₁-Benzyl-Substituted Oxadiazoles. To a solution of **14** (0.25 g, 0.79 mmol) in anhydrous DMF (5 mL) was added cesium carbonate (0.78 g, 2.4 mmol), which was stirred for 30 min. The benzyl halide was then added (2.0 mmol), and the resulting solution was stirred overnight at room temperature under nitrogen. The solvent was removed in vacuo and the crude residue dissolved in ethyl acetate (20 mL). The organic phase was washed with water (20 mL) and brine (20 mL) and dried over magnesium sulfate. The solvent was removed in vacuo to give the crude product. Unless otherwise stated, the crude compounds were purified using column chromatography, eluting with 4:1 cyclohexane/ethyl acetate.

tert-Butyl 5-(1-Benzyl-1*H*-indazol-3-yl)-1,2,4-oxadiazol-3-yl)methylcarbamate (15). White powder (0.11 g, 34%); mp 80–81 °C; δ_{H} (300 MHz, CDCl₃) 1.48 (9H, s, (O'Bu), 4.61 (2H, d *J* 5.4 Hz, CH₂NH), 5.75 (2H, s, NCH₂), 6.71–7.46 (5H, m, ArH), 8.31 (1H, d *J* 8.3 Hz, ArH); δ_{C} (75.5 MHz, CDCl₃) 171.4, 168.4, 162.6, 155.6, 140.5, 135.4, 130.0, 128.0, 127.6, 127.4, 123.7, 123.0, 121.6, 110.3, 80.1, 54.2, 36.5, 28.2; LC-MS-EI 406.4 (MH⁺, 100); found (CI) 406.187 02. C₂₂H₂₃N₅O₃ (MH⁺) requires 406.187 91. Anal. Calcd for C₂₂H₂₃N₅O₃: C, 65.17; H, 5.72; N, 17.27. Found C, 65.09; H, 5.96; N, 17.06.

General Method for the Mitsunobu Synthesis of the N₂-Benzyl-Substituted Oxadiazoles. To a solution of **14** (0.25 g, 0.79 mmol), under nitrogen, in toluene (10 mL), benzyl alcohol (0.87 mmol), tributylphosphine (0.26 g, 0.31 mL, 1.26 mmol), and TMAD (0.22 g, 1.26 mmol) were added successively. The resulting clear-yellow solution was allowed to stir overnight at room temperature. The solution was then extracted with water, 1 N HCl, 1 N sodium hydroxide (aq), and brine. The combined aqueous phases were washed with dichloromethane and the combined organic phases dried over magnesium sulfate. The solvent was removed in vacuo.

Unless otherwise stated, the crude compounds were purified using column chromatography (4:1 cyclohexane/ethyl acetate).

tert-Butyl 5-(2-Benzyl-2*H*-indazol-3-yl)-1,2,4-oxadiazol-3-yl)methylcarbamate (16). The compound was purified by recrystallizing from methanol to give a white powder (0.09 g, 28%) or alternatively column chromatography using 2:1 cyclohexane/ethyl acetate: mp 153–154 °C; δ_{H} (300 MHz, CDCl₃) 1.49 (9H, s, (O'Bu), 4.60 (2H, d *J* 5.8 Hz, CH₂NH), 6.23 (2H, s, NCH₂), 7.30–7.43 (7H, m, ArH), 7.86 (1H, d *J* 8.4 Hz, ArH), 8.19 (1H, d *J* 8.2 Hz, ArH); δ_{C} (75.5 MHz, CDCl₃) 168.3, 168.2, 156.3, 148.2, 135.7, 128.9, 128.6, 128.2, 127.9, 127.1, 125.8, 123.5, 120.5, 119.0, 118.5, 81.4, 56.6, 53.4, 28.3; LC-MS-EI 406.4 (MH⁺, 100); found (EI) 405.179 40. C₂₂H₂₃N₅O₃ (M) requires 405.180 08.

General Method for the Deprotection of the Boc-Protected Oxadiazoles. The boc-protected oxadiazoles (0.03 g–0.25 g) were dissolved in trifluoroacetic acid (1.9 mL, 95%), and then triisopropylsilane (0.05 mL, 2.5%) and water (0.05 mL, 2.5%) were added. The solution was allowed to stir for 18 h at room temperature. Ice-cold diisopropyl ether or diethyl ether was added until a white precipitate started to form. The white precipitate was then filtered off and allowed to dry.

(5-(1-Benzyl-1*H*-indazol-3-yl)-1,2,4-oxadiazol-3-yl)methanamine (11). White powder (60 mg, >99%); mp 118–119 °C; δ_{H} (300 MHz, MeOH- d_4) 4.39 (2H, s, CH₂NH₂), 5.82 (2H, s, NCH₂), (8H, m, ArH), 8.31 (1H, d *J* 8.3 Hz, ArH); δ_{C} (75.5 MHz, MeOH- d_4) 173.1, 166.6, 142.1, 137.3, 130.4, 129.9, 129.2, 129.0, 128.6, 125.1, 124.2, 122.2, 112.0, 54.8, 36.1; LC-MS-EI 306.4 (MH⁺, 100); found (CI) 306.135 01. C₁₇H₁₅N₅O (MH⁺) requires 306.135 48. Anal. Calcd for C₁₇H₁₅N₅O: C, 66.87; H, 4.95; N, 22.94. Found: C, 67.00; H, 4.82; N, 22.97.

(5-(2-Benzyl-2*H*-indazol-3-yl)-1,2,4-oxadiazol-3-yl)methanamine (38). White powder (96 mg, 98%); mp 144–145 °C; δ_{H} (300 MHz, MeOH- d_4) 4.48 (2H, t *J* Hz, CH₂NH₂), 6.22 (2H, t *J* Hz, NCH₂), 7.29–7.47 (7H, m, ArH), 7.80 (1H, m, ArH), 8.18 (1H, m, ArH); δ_{C} (75.5 MHz, MeOH- d_4) 170.3, 166.4, 149.5, 137.4, 129.8, 129.2, 128.6, 127.3, 124.8, 121.4, 120.0, 119.4, 57.6, 36.0; LC-MS-EI 306.4 (MH⁺, 75); found (CI) 306.135 54. C₁₇H₁₅N₅O (MH⁺) requires 306.135 48.

Biological Methods. Preparation of Rat Forebrain Synaptosomes and Homogenates. Experiments were performed using forebrain (whole brain less cerebellum/medulla) from male Wistar rats weighing 175–250 g. All efforts were made to reduce the number of animals used, and all experiments were carried out in accordance with the U.K. Animals (Scientific Procedures) Act, 1986, and the European Community Council Directive of November 24, 1986 (86/609/EEC). Following killing of animals by stunning and decapitation, the forebrain was rapidly dissected and transferred to a weighed tube containing ice-cold 0.25 M sucrose.

Synaptosomes (heavy and light mitochondrial fraction containing synaptosomes) were prepared by transferring the forebrain (of known wet weight) to a glass Potter vessel to which 9 volumes of ice-cold 0.25 M sucrose had been added and homogenizing, using a Teflon pestle, by 8 “up and down strokes” of a Braun Potter S motor driven homogenizer set to 900 rpm. The resulting homogenate was centrifuged at 1036g at 4 °C for 10 min and the supernatant collected. The remaining pellet was resuspended, as above, in fresh ice-cold 0.25 M sucrose and the centrifugation step repeated. The supernatant fractions were pooled and centrifuged at 40000g (average) at 4 °C for 15 min and the resulting pellet resuspended in the appropriate assay buffer at a concentration of 20–25 mg wet weight per mL of appropriate assay buffer.

Homogenates were prepared by transferring the known weight of forebrain to a cooled tube containing 9 volumes of ice-cold 50 mM HEPES buffer, pH 7.4. The mixture was homogenized at 4 °C using 3 × 5 s bursts of an Ultra-Turrax homogenizer set at maximum speed. The resulting homogenate was centrifuged at 40000g (average) at 4 °C for 15 min and the supernatant discarded. The resulting pellet was resuspended in 9 volumes of fresh ice-cold pH 7.4 buffer (as above), the centrifugation step was repeated and the resulting pellet resuspended in the appropriate assay buffer at a concentration of 20–25 mg wet weight per mL.

Table 8

relative importance	descriptor
0.313 092	weinerPath (Wiener path: half the sum of all distance matrix entries)
0.109 397	TPSA (polar surface area calculated from group contributions to approximate the polar surface area from connection table)
0.302 393	Diameter (largest value in the distance matrix)
0.199 622	a_count (number of atoms. This is calculated as the sum of (1 + hi) over all nontrivial atoms i.)
0.357 376	b_count (number of bonds. This is calculated as the sum of (di/2 + hi) over all nontrivial atoms i.)
0.457 179	vsa_acc (approximation of the sum of VDW surface areas of pure hydrogen bond acceptors (not counting acidic atoms and atoms that are both hydrogen bond donors and acceptors such as -OH)
0.506 421	vsa_pol (approximation to the sum of VDW surface areas of polar atoms (atoms that are both hydrogen bond donors and acceptors), such as -OH)
0.841 705	ASA (water accessible surface area calculated using a radius of 1.4 Å for the water molecule)
0.897 918	vdw_vol (van der Waals volume calculated using a connection table approximation)
1.000 000	vol (van der Waals volume calculated using a grid approximation)

[¹⁴C]Guanidine Flux. Assays were carried out using 14 mL polypropylene test tubes to which a range of concentrations of the compounds under test were added. Test compounds were dissolved in DMSO and added to assays such that the maximum concentration of DMSO did not exceed 2% v/v. Compounds under test were preincubated for 10 min at 30 °C in incubation buffer (50 mM HEPES adjusted to pH 7.4 with Tris base, 130 mM choline chloride, 5.5 mM D-glucose, 0.8 mM MgSO₄, and 5 mM KCl) containing 7.5 mg of original wet weight of tissue and 100 μg of veratrine HCl in a final volume of 0.5 mL. Uptake was initiated by the addition of 0.5 mL of [¹⁴C]guanidine (1.0 μCi/mL in incubation buffer) and terminated 2.5 min later by the addition of 10 mL of ice-cold wash buffer (163 mM choline chloride, 1.8 mM CaCl₂, and 0.8 mM MgSO₄ in 5 mM HEPES buffer, pH 7.4), followed immediately by vacuum filtration through Whatman GF/C glass fiber filters using a Brandel cell harvester. A further 2 × 5 mL of ice-cold wash buffer was added to each tube and the vacuum filtration step repeated. The GF/C glass fiber filters were transferred to minivials and 4 mL of Picofluor⁴⁰ liquid scintillant added using a Brandel deposit/dispense system. Radioactivity was measured using a Beckman liquid scintillation counter.

Computation of IC₅₀ Values. Data are presented as mean values ± sem, with the number of experiments indicated in brackets. IC₅₀ values were obtained from radioligand displacement or guanidine flux inhibition curves by plotting log₁₀ concentration vs bound ligand/guanidine uptake according the equation

$$y = R_{\min} + \frac{R_{\text{sp}}}{1 + \exp[-n(x - C)]}$$

where y = bound (dpm), x = log₁₀ compound concentration, R_{\min} = lower asymptote (i.e., 100% inhibition), R_{sp} = upper asymptote - R_{\min} (i.e., specific binding), n = slope (log₁₀), and C = IC₅₀ (the concentration required to inhibit 50% of specific binding).

Hippocampal Slice Assay. Following killing of animals by stunning and decapitation, the forebrain (whole brain less cerebellum/medulla) was rapidly dissected and transferred to a vessel containing ice-cold pregassed, artificial cerebral spinal fluid (aCSF). Hippocampi were rapidly dissected and 0.4 mm slices prepared using a McIlwain tissue chopper. Slices were randomly distributed in 50 mL conical flasks containing 25–30 mL of ice-cold pregassed aCSF. Flasks were incubated at 30 °C for 30 min under continued gassing with 95% O₂/5% CO₂. The medium was then removed by vacuum aspiration and fresh aCSF added, and slices were incubated for a further 30 min. Medium was again removed by vacuum aspiration and replaced by exactly 25 mL of prewarmed (30 °C) Ca²⁺-free aCSF containing compounds under test. Following a further 10 min of incubation under continuous gassing, two to three slices were removed (in a volume of 100 μL using an

Eppendorf pipet) for measurement of ATP and protein by immediate transfer to individual microfuge tubes containing 0.4 mL of ice-cold 0.5 M trichloroacetic acid (TCA). Iodoacetate (25 μL of a 0.4 M solution) was added to the remaining flasks, and gassing discontinued. Exactly 11 min later, three to four slices were removed and transferred to microfuge tubes containing TCA (as above) for measurement of ATP and protein.

Measurement of ATP and Protein. Individual slices were disrupted by ultrasonication and the resulting homogenates centrifuged at 10 000 rpm for 5 min at 4 °C. The supernatant was decanted into a fresh tube and any remaining supernatant removed by vacuum aspiration. The pellet was resuspended in 0.5 mL of 0.1 M KOH by ultrasonication, and the resulting suspensions warmed with gentle agitation at 37 °C for 30 min.

Concentrations of ATP were measured in 6 μL of supernatant by mixing with Luciferase reagent (ATPLite from Perkin-Elmer) and measuring subsequent luminescence in a 96-well plate counter. Protein concentrations were measured using BCA protein assay (Pierce) with bovine serum albumin as standard. ATP concentrations were expressed as nmol/mg protein and neuroprotective indices (% protection) calculated by direct comparison within each experiment with the effect of 1 μM tetrodotoxin.

Electrophysiological Methods. Hippocampal slices from P14–16 Sprague–Dawley rats were cut at a thickness of 0.3 mm and maintained in carbogenated aCSF. Slices were chemically treated with protease XIII for 10 min at 37 °C in PIPES buffer solution containing (in mM) PIPES 86, NaCl 30, KCl 3, MgCl₂ 2, and glucose 10 and adjusted to pH 7.4 (using NaOH) and an osmolarity of 290–300 mOsm. To inhibit the protease, protease XXIII inhibitor and bovine albumin were added to extracellular recording solution containing (in mM) NaCl 80, tetraethylammonium chloride 60, KCl 2.5, MgCl₂ 1.3, CaCl₂ 0.5, CdCl₂ 0.1, glucose 11, and HEPES 5, adjusted to pH 7.4 (using NaOH) and to an osmolarity of ~290 mOsm. The CA1 region was dissected from the slice and triturated to mechanically break down the tissue, using firepolished pipettes. The cell suspension was placed on poly-D-lysine coated glass coverslips to aid cell adhesion and left to settle for 20 min before beginning recordings.

Whole-cell voltage recordings were made from neurons lacking prominent processes (to eliminate space-clamp problems) using electrodes of 1.8–2.5 MΩ. They were backfilled with whole-cell recording solution that contained (in mM) CsF 120, CsEGTA 10, NaCl 10, and HEPES 10, adjusted to pH 7.40 (using NaOH) and to an osmolarity of ~290 mOsm (using CsF).

Current–voltage relationships were used to assess the validity of the voltage-clamp recordings. Cells were used if the peak current was close to -10 mV and showed a graded activation. Inward currents were completely blocked by tetrodotoxin (1 μM).

Na_v Isoform Screening. All compounds were dissolved in DMSO to make 1 mM or 10 mM stock solutions and diluted with assay buffer. In the voltage-sensitive dye experiments, screening of compounds against human Na_v isoforms 1.1, 1.3, 1.4, 1.5, 1.6, 1.7, and 1.8 was conducted by Scottish Biomedical Ltd., Glasgow, U.K. Briefly, the individual isoforms were stably expressed in HEK293 cells together with the β1 subunit, except for Na_v1.8 where no β subunit was used. Cells were checked for sensitivity to tetrodotoxin (1.5 and 1.8 were tetrodotoxin-resistant). Testing was performed using the membrane potential assay kit from Molecular Devices. Patch-clamp experiments against Na_v1.2 and Na_v1.6 were performed by Chantest Inc., Cleveland, OH. Briefly, test compounds were evaluated at room temperature using the PatchXpress 7000A (Molecular Devices), an automatic parallel patch-clamp system. Compounds were evaluated at 10 and 50 μM, except for lamotrigine on Na_v1.2, where the concentrations were 30 and 100 μM, each concentration being tested in two to four cells. The duration of each exposure was 5 min. Use-dependence of inhibition on hNa_v1.2 and hNa_v1.6 was determined using a double pulse protocol. A holding potential of -80 mV and prepulse potential of -120 mV were followed by pulse 1-0 mV for 200 ms. An interpulse potential of -80 mV was then applied for 200 ms, followed by a second pulse of 0 mV for 20 ms. The pulse pattern was repeated at 10 s intervals (0.1 Hz), and peak current amplitudes at both test pulses were measured. Percentage use-dependent inhibition (I) was calculated from the equation $I = (1 - P_{2T}/P_{1T}) \times P_{1C}/P_{2C} \times 100$, where P1 and P2 refer to the current amplitudes produced by the first and second pulses, respectively, and subscripts T and C refer to test and control conditions.

QSAR Descriptors. Table 8 shows the relative importance of selected subset of descriptors used to calculate the correlation plot in Figure 1b.

Acknowledgment. The authors thank UCL Business, the Bloomsbury Bioseed Fund, ProAxon Ltd., The Sir Jules Thorn Charitable Trust, and The Wellcome Trust for financial support and Salvador Moncada for helpful discussions and advice.

Supporting Information Available: ¹H NMR, ¹³C NMR, and HRMS data for additional compounds, QSAR descriptors, and LCMS data. This material is available free of charge via the Internet at <http://pubs.acs.org>.

References

- Catterall, W. A. Structure and function of voltage-gated ion channels. *Annu. Rev. Biochem.* **1995**, *64*, 493-531.
- Catterall, W. A. From ionic currents to molecular mechanisms: the structure and function of voltage-gated sodium channels. *Neuron* **2000**, *26*, 13-25.
- Tarnawa, I.; Bolskei, H.; Kocsis, P. Blockers of voltage-gated sodium channels for the treatment of central nervous system diseases. *Recent Pat. CNS Drug Discovery* **2007**, *2*, 57-78.
- Clare, J. J.; Tate, S. N.; Nobbs, M.; Romanos, M. A. Voltage-gated sodium channels as therapeutic targets. *Drug Discovery Today* **2000**, *5*, 506-520.
- Perucca, E.; French, J.; Bialer, M. Development of new antiepileptic drugs: challenges, incentives, and recent advances. *Lancet Neurol.* **2007**, *9*, 793-804.
- Choi, H.; Morrell, M. J. Review of lamotrigine and its clinical applications in epilepsy. *Expert Opin. Pharmacother.* **2003**, *4*, 243-251.
- Ambrosio, A. F.; Soares-Da-Silva, P.; Carvalho, C. M.; Carvalho, A. P. Mechanisms of action of carbamazepine and its derivatives, oxcarbazepine, BIA 2-093, and BIA 2-024. *Neurochem. Res.* **2002**, *27*, 121-130.
- Wood, J. N.; Boorman, J. Voltage-gated sodium channel blockers: target validation and therapeutic potential. *Curr. Top. Med. Chem.* **2005**, *5*, 529-537.
- Baker, M. D.; Wood, J. N. Involvement of Na⁺ channels in pain pathways. *Trends Pharmacol. Sci.* **2001**, *22*, 27-31.
- Lai, J.; Hunter, J. C.; Porreca, F. The role of voltage-gated sodium channels in neuropathic pain. *Curr. Opin. Neurobiol.* **2003**, *13*, 291-297.
- Amir, R.; Argoff, C. E.; Bennett, G. J.; Cummins, T. R.; Durieux, M. E.; Gerner, P.; Gold, M. S.; Porreca, F.; Strichartz, G. R. The role of sodium channels in chronic inflammatory and neuropathic pain. *J. Pain* **2006**, *7*, S1-S29.
- Sindrup, S. H.; Jensen, T. S. Efficacy of pharmacological treatments of neuropathic pain: an update and effect related to mechanism of drug action. *Pain* **1999**, *83*, 389-400.
- Backonja, M. Anticonvulsants for the treatment of neuropathic pain syndromes. *Curr. Pain Headache Rep.* **2003**, *7*, 39-42.
- Jensen, T. S. Anticonvulsants in neuropathic pain: rationale and clinical evidence. *Eur. J. Pain* **2002**, *6*, 61-68.
- Veneroni, O.; Maj, R.; Calabresi, M.; Faravelli, L.; Fariello, R. G.; Salvati, P. Anti-allodynic effect of NW-1029, a novel Na⁽⁺⁾ channel blocker, in experimental animal models of inflammatory and neuropathic pain. *Pain* **2003**, *102*, 17-25.
- Mao, J.; Chen, L. L. Systemic lidocaine for neuropathic pain relief. *Pain* **2000**, *87*, 7-17.
- Kyle, D. J.; Ilyin, V. I. Sodium channel blockers. *J. Med. Chem.* **2007**, *50*, 2583-2588.
- Nassar, M. A.; Baker, M. D.; Levato, A.; Ingram, R.; Mallucci, G.; McMahon, S. B.; Wood, J. N. Nerve injury induces robust allodynia and ectopic discharges in Nav1.3 null mutant mice. *Mol. Pain* **2006**, *2*, 33.
- Waxman, S. G. Mechanisms of disease: sodium channels and neuroprotection in multiple sclerosis—current status. *Nat. Clin. Pract. Neurol.* **2008**, *4*, 159-169.
- Tymianski, M.; Tator, C. H. Normal and abnormal calcium homeostasis in neurons: a basis for the pathophysiology of traumatic and ischemic central nervous system injury. *Neurosurgery* **1996**, *38*, 1176-1195.
- Wolf, P. A.; Cobb, J. L.; D'Agostino, R. B. *Stroke Pathophysiology, Diagnosis, and Management*; W.B. Saunders: Philadelphia, PA, 1998.
- Green, A. R.; Shuaib, A. Therapeutic strategies for the treatment of stroke. *Drug Discovery Today* **2006**, *11*, 681-693.
- Squire, I. B.; Lees, K. R.; Pryse-Phillips, W.; Kertesz, A.; Bamford, J. Efficacy and tolerability of lifarizine in acute ischemic stroke. A pilot study. Lifarizine Study Group. *Ann. N.Y. Acad. Sci.* **1995**, *765*, 317-318.
- Diener, H. C.; Hacke, W.; Hennerici, M.; Radberg, J.; Hantson, L.; De, K. J. Lubeluzole in acute ischemic stroke. A double-blind, placebo-controlled phase II trial. Lubeluzole International Study Group. *Stroke* **1996**, *27*, 76-81.
- Muir, K. W.; Holzapfel, L.; Lees, K. R. Phase II clinical trial of sipatrigine (619C89) by continuous infusion in acute stroke. *Cerebrovasc. Dis.* **2000**, *10*, 431-436.
- Cheng, Y. D.; Al-Khoury, L.; Zivin, J. A. Neuroprotection for ischemic stroke: two decades of success and failure. *NeuroRx* **2004**, *1*, 36-45.
- De, K. J.; Sulter, G.; Luiten, P. G. Clinical trials with neuroprotective drugs in acute ischaemic stroke: are we doing the right thing? *Trends Neurosci.* **1999**, *22*, 535-540.
- Bensimon, G.; Doble, A. The tolerability of riluzole in the treatment of patients with amyotrophic lateral sclerosis. *Expert Opin. Drug Saf.* **2004**, *3*, 525-534.
- Stocchi, F.; Arnold, G.; Onofri, M.; Kwiecinski, H.; Szczudlik, A.; Thomas, A.; Bonuccelli, U.; Van, D. A.; Cattaneo, C.; Sala, P.; Fariello, R. G. Improvement of motor function in early Parkinson disease by safinamide. *Neurology* **2004**, *63*, 746-748.
- Kapoor, R. Sodium channel blockers and neuroprotection in multiple sclerosis using lamotrigine. *J. Neurol. Sci.* **2008**, *274*, 54-56.
- Garthwaite, G.; Goodwin, D. A.; Neale, S.; Riddall, D.; Garthwaite, J. Soluble guanylyl cyclase activator YC-1 protects white matter axons from nitric oxide toxicity and metabolic stress, probably through Na⁽⁺⁾ channel inhibition. *Mol. Pharmacol.* **2002**, *61*, 97-104.
- Waxman, S. G. Axonal conduction and injury in multiple sclerosis: the role of sodium channels. *Nat. Rev. Neurosci.* **2006**, *7*, 932-941.
- Anger, T.; Madge, D. J.; Mulla, M.; Riddall, D. Medicinal chemistry of neuronal voltage-gated sodium channel blockers. *J. Med. Chem.* **2001**, *44*, 115-137.
- Unverferth, K.; Engel, J.; Hofgen, N.; Rostock, A.; Gunther, R.; Lankau, H. J.; Menzer, M.; Rolfs, A.; Liebscher, J.; Muller, B.; Hofmann, H. J. Synthesis, anticonvulsant activity, and structure-activity relationships of sodium channel blocking 3-aminopyrroles. *J. Med. Chem.* **1998**, *41*, 63-73.
- Lankau, H. J.; Unverferth, K.; Grunwald, C.; Hartenhauer, H.; Heinecke, K.; Bernoster, K.; Dost, R.; Egerland, U.; Rundfeldt, C. New GABA-modulating 1,2,4-oxadiazole derivatives and their anti-convulsant activity. *Eur. J. Med. Chem.* **2007**, *42*, 873-879.
- Rishton, G. M. Nonleadlikeness and leadlikeness in biochemical screening. *Drug Discovery Today* **2003**, *8*, 86-96.
- Selwood, D. L.; Brummell, D. G.; Budworth, J.; Burtin, G. E.; Campbell, R. O.; Chana, S. S.; Charles, I. G.; Fernandez, P. A.; Glen, R. C.; Goggin, M. C.; Hobbs, A. J.; Kling, M. R.; Liu, Q.; Madge, D. J.; Meilleris, S.; Powell, K. L.; Reynolds, K.; Spacey, G. D.; Stables, J. N.; Tatlock, M. A.; Wheeler, K. A.; Wishart, G.; Woo,

- C. K. Synthesis and biological evaluation of novel pyrazoles and indazoles as activators of the nitric oxide receptor, soluble guanylate cyclase. *J. Med. Chem.* **2001**, *44*, 78–93.
- (38) Lu, J. J.; Crimin, K.; Goodwin, J. T.; Crivori, P.; Orrenius, C.; Xing, L.; Tandler, P. J.; Vidmar, T. J.; Amore, B. M.; Wilson, A. G.; Stouten, P. F.; Burton, P. S. Influence of molecular flexibility and polar surface area metrics on oral bioavailability in the rat. *J. Med. Chem.* **2004**, *47*, 6104–6107.
- (39) Kayukova, L. Synthesis of 1,2,4-oxadiazoles (a review). *Pharm. Chem. J.* **2005**, *39*, 539–547.
- (40) Sureshbabu, V. V.; Hemantha, H. P.; Naik, S. A. Synthesis of 1,2,4-oxadiazole-linked orthogonally urethane-protected dipeptide mimetics. *Tetrahedron Lett.* **2008**, *49*, 5133–5136.
- (41) Santagada, V.; Frecentese, F.; Perissutti, E.; Cirillo, D.; Terracciano, S.; Caliendo, G. A suitable 1,2,4-oxadiazoles synthesis by microwave irradiation. *Bioorg. Med. Chem. Lett.* **2004**, *14*, 4491–4493.
- (42) Evans, M. D.; Ring, J.; Schoen, A.; Bell, A.; Edwards, P.; Berthelot, D.; Nicewonger, R.; Baldino, C. M. The accelerated development of an optimized synthesis of 1,2,4-oxadiazoles: application of microwave irradiation and statistical design of experiments. *Tetrahedron Lett.* **2003**, *44*, 9337–9341.
- (43) Tsunoda, T.; Otsuka, J.; Yamamiya, Y.; Itô, S. *N,N,N',N'*-Tetramethylazodicarboxamide (TMAD), a new versatile reagent for Mitsunobu reaction. Its application to synthesis of secondary amines. *Chem. Lett.* **1994**, *23*, 539–542.
- (44) Pauwels, P. J.; Leysen, J. E.; Laduron, P. M. [³H]Batrachotoxinin A 20- α -benzoate binding to sodium channels in rat brain: characterization and pharmacological significance. *Eur. J. Pharmacol.* **1986**, *124*, 291–298.
- (45) Riddall, D. R.; Leach, M. J.; Garthwaite, J. A novel drug binding site on voltage-gated sodium channels in rat brain. *Mol. Pharmacol.* **2006**, *69*, 278–287.
- (46) Fowler, J. C.; Li, Y. Contributions of Na⁺ flux and the anoxic depolarization to adenosine 5'-triphosphate levels in hypoxic/hypoglycemic rat hippocampal slices. *Neuroscience* **1998**, *83*, 717–722.
- (47) Lin, A. QuaSAR-Descriptor, Molecular Operating Environment. <http://www.chemcomp.com>, 2007.
- (48) Trezise, D. J.; John, V. H.; Xie, X. M. Voltage- and use-dependent inhibition of Na⁺ channels in rat sensory neurones by 4030W92, a new antihyperalgesic agent. *Br. J. Pharmacol.* **1998**, *124*, 953–963.
- (49) Xie, X. M.; Garthwaite, J. State-dependent inhibition of Na⁺ currents by the neuroprotective agent 619C89 in rat hippocampal neurons and in a mammalian cell line expressing rat brain type IIA Na⁺ channels. *Neuroscience* **1996**, *73*, 951–962.
- (50) Xie, X.; Lancaster, B.; Peakman, T.; Garthwaite, J. Interaction of the antiepileptic drug lamotrigine with recombinant rat brain type IIA Na⁺ channels and with native Na⁺ channels in rat hippocampal neurones. *Pfluegers Arch.* **1995**, *430*, 437–446.
- (51) Jarnot, M.; Corbett, A. M. Immunolocalization of Nav1.2 channel subtypes in rat and cat brain and spinal cord with high affinity antibodies. *Brain Res.* **2006**, *1107*, 1–12.
- (52) Blumenfeld, H.; Lampert, A.; Klein, J. P.; Mission, J.; Chen, M. C.; Rivera, M.; Dib-Hajj, S.; Brennan, A. R.; Hains, B. C.; Waxman, S. G. Role of hippocampal sodium channel Nav1.6 in kindling epileptogenesis. *Epilepsia* **2008**, *50*, 44–55.
- (53) Lindia, J. A.; Abbadie, C. Distribution of the voltage gated sodium channel Na(v)1.3-like immunoreactivity in the adult rat central nervous system. *Brain Res.* **2003**, *960*, 132–141.
- (54) Guo, F.; Yu, N.; Cai, J. Q.; Quinn, T.; Zong, Z. H.; Zeng, Y. J.; Hao, L. Y. Voltage-gated sodium channel Nav1.1, Nav1.3 and beta1 subunit were up-regulated in the hippocampus of spontaneously epileptic rat. *Brain Res. Bull.* **2008**, *75*, 179–187.
- (55) Drizin, I.; Gregg, R. J.; Scanio, M. J. C.; Shi, L.; Gross, M. F.; Atkinson, R. N.; Thomas, J. B.; Johnson, M. S.; Carroll, W. A.; Marron, B. E.; Chapman, M. L.; Liu, D.; Krambis, M. J.; Shieh, C. C.; Zhang, X.; Hernandez, G.; Gauvin, D. M.; Mikusa, J. P.; Zhu, C. Z.; Joshi, S.; Honore, P.; Marsh, K. C.; Roeloffs, R.; Werness, S.; Krafte, D. S.; Jarvis, M. F.; Faltynek, C. R.; Kort, M. E. Discovery of potent furan piperazine sodium channel blockers for treatment of neuropathic pain. *Bioorg. Med. Chem.* **2008**, *16*, 6379–6386.
- (56) Fraser, R. A.; Sherrington, R.; Macdonald, M. L.; Samuels, M.; Newman, S.; Fu, J. M.; Kamboj, R. Potent and Selective Nav1.7 Sodium Channel Blockers. PCT/US2007/00725 [WO/2007/109324], 2007.
- (57) Hains, B. C.; Saab, C. Y.; Waxman, S. G. Changes in electrophysiological properties and sodium channel Nav1.3 expression in thalamic neurons after spinal cord injury. *Brain* **2005**, *128*, 2359–2371.
- (58) Obach, R. S.; Walsky, R. L.; Venkatakrishnan, K.; Gaman, E. A.; Houston, J. B.; Tremaine, L. M. The utility of in vitro cytochrome P450 inhibition data in the prediction of drug–drug interactions. *J. Pharmacol. Exp. Ther.* **2006**, *316*, 336–348.
- (59) Benet, L. Z.; Kroetz, D. L.; Sheiner, L. B. Pharmacokinetics: The Dynamics of Drug Absorption Distribution and Elimination. In *Goodman & Gilman's The Pharmacological Basis of Therapeutics*; McGraw-Hill, Health Professions Division: New York, 1996; pp 3–27.
- (60) Scheuer, T.; Catterall, W. A. Control of neuronal excitability by phosphorylation and dephosphorylation of sodium channels. *Biochem. Soc. Trans.* **2006**, *34*, 1299–1302.

JM801180P